In NPAR 2007

Highlight Lines for Conveying Shape

Doug DeCarlo
Rutgers University

Szymon Rusinkiewicz
Princeton University

C + SC + PH + SH C + SC + PH C + S

Toon shading 存在问题：
轮廓变得模糊，shape不是很明确
highlight lines + dark lines 来显示结构信息
white line to convey shape

Figure 1: *David's head with different types of highlight lines (and a toon shader)*

Abstract

Recent work has shown that sparse lines defined on 3D shapes, including occluding contours and suggestive contours, are effective at conveying shape. We introduce two new families of lines called *suggestive highlights* and *principal highlights*, based on definitions related to suggestive contours and geometric creases. We show that when these are drawn in white on a gray background they are naturally interpreted as highlight lines, and complement contours and suggestive contours. We provide object-space definitions and algorithms for extracting these lines, explore several stylization possibilities, and compare the lines to ridges and valleys of intensity in diffuse-shaded images.

Keywords: non-photorealistic rendering, line drawings, highlights

1 Introduction

Our visual system is remarkably effective at reconstructing a 3D shape given just a sparse set of lines on the surface, such as occluding contours and suggestive contours. It seems that line drawings can be effective as long as they give *some* evidence about how a shape behaves. It is not always easy to provide that evidence, however. In elliptical regions of the shape, for example, there are no suggestive contours, and depending on the viewpoint there may be no occluding contours either. However, we would still like to be able to include markings in a line drawing that suggest the bulge or indentation. Shading provides another challenge: the dark fills created by techniques such as toon shading will obscure suggestive contours and other dark lines drawn to suggest detail, in regions where the shape is shaded. In this paper, we propose to address both of these problems by drawing *highlight lines* in light colors over dark backgrounds.

木炭和白粉笔

We are motivated by artistic styles that supplement dark lines with highlights by drawing with charcoal and white chalk. This yields highlights but rarely lines; rubbing and smudging in chalk lets artists easily fill regions of the image. However, we have been inspired by a number of artists that do use white lines effectively to convey shape—particularly the work of Frank Miller (Figure 9) and Roy Lichtenstein (Figure 12).

Our strategy is to build upon the framework of suggestive contours [DeCarlo et al. 2003; DeCarlo et al. 2004] to characterize 3D linear features on surfaces that can be effectively rendered in white on dark backgrounds. Recall that suggestive contours are essentially a mathematical exaggeration of occluding contours: they anticipate the appearance of contours in nearby viewpoints. Drawing these lines also serves to abstract an image produced by diffuse-shading the object using a light located at the camera (shading based on $\hat{\mathbf{n}} \cdot \hat{\mathbf{v}}$, where $\hat{\mathbf{n}}$ is the normal and $\hat{\mathbf{v}}$ is the view direction). This is reflected by the definition of suggestive contours as being minima of $\hat{\mathbf{n}} \cdot \mathbf{v}$ in the projected view direction, and also by the observation that suggestive contours seem to closely approximate valleys of intensity in such images (which was the justification for the image-space algorithm for suggestive contours in [DeCarlo et al. 2003]). So, suggestive contours abstract the darkest regions of the image by representing them with lines. We extend the abstraction by depicting the brightest regions of the image—the highlights—with lines, an approach independently proposed by Lee et al. [2007]. We draw such lines in white (against a darker background). See Figure 1.

Contours or suggestive contours最小值n*v
Principle highlight or suggestive highlight 最大值n*v

In this paper, we argue that highlight lines are described by two types of lines: suggestive highlights (which appear at view-dependent inflections) and principal highlights (which appear when the surface is viewed along a principal curvature direction). We will demonstrate that these lines are *maxima* of $\hat{\mathbf{n}} \cdot \mathbf{v}$ in specific directions, and present definitions of these lines in terms of local surface geometry. We continue by describing algorithms for their extraction, and effective rendering styles that include them.

2 Related Work

Our approach defines new geometric linear features of the *surface*. There are a number of such lines that serve as ingredients in non-photorealistic renderings of shape. They include occluding contours (interior and exterior silhouettes — locations at which the surface normal is perpendicular to the view direction) [Elber and Cohen 1990; Winkenbach and Salesin 1994; Markosian et al. 1997; Hertzmann and Zorin 2000], sharp creases [Gooch et al. 1999; Markosian et al. 1997; Saito and Takahashi 1990], ridge and valley lines (local maxima of principal curvature magnitude in a principal direction) [Interrante et al. 1995; Thirion and Gourdon 1996; Pauly et al. 2003; Ohtake et al. 2004], apparent ridges (variants of geometric ridges that include a view-dependent projection) [Judd et al. 2007], and suggestive contours (locations at which occluding contours appear with minimal change in viewpoint) [DeCarlo et al. 2003; DeCarlo et al. 2004]. Such lines are typically drawn in black on a lighter background, although they are sometimes drawn in white. For instance, sharp creases that are not on the contour are drawn in white by Gooch et al. [1999] to depict highlights. To our knowledge, the two new types of highlight lines defined here represent the first such object-space description of these lines on smooth surfaces. Other styles are possible as well, including non-photorealistic illustration of specular reflections of the environment [Weidenbacher et al. 2006].

We also compare our results to an image-space algorithm that works from a rendered image, an approach related to the image-space and depth-buffer processing performed by Saito and Takahashi [1990], the image-space algorithm for suggestive contours [DeCarlo et al. 2003], and the GPU algorithm of Lee et al. [2007]. This is also related to processing of photographs into line drawings [Pearson and Robinson 1985; Iverson and Zucker 1995].

3 Highlight Lines

This section assumes familiarity with the definitions of suggestive contours [DeCarlo et al. 2003], although some material is summarized here. We start by defining the contour and suggestive contour.

Consider a smooth, closed surface that is viewed from a point $\mathbf{c}$. For any point $\mathbf{p}$ on the surface, the viewing direction is defined as $\mathbf{v} = \mathbf{c} - \mathbf{p}$. The occluding contour [Cipolla and Giblin 2000] is the boundary between the visible and hidden parts of the surface. It is generated by the set of points where the surface is viewed edge-on, where the normal vector $\hat{\mathbf{n}}$ is perpendicular to the viewing direction:

$$\hat{\mathbf{n}} \cdot \hat{\mathbf{v}} = 0. \tag{1}$$

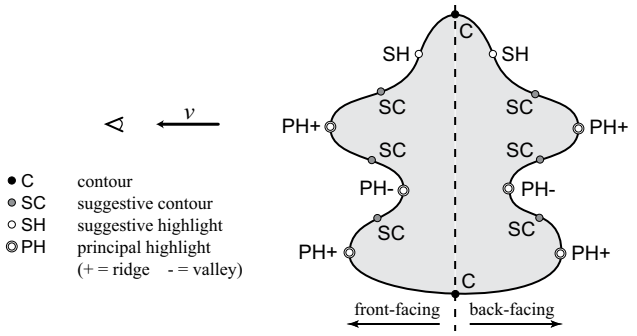

Figure 2: *Different types of lines given the viewing direction v (for clarity this figure uses orthographic projection, hence constant v).*

(Here, unit vectors are denoted with hats, so that $\hat{\mathbf{v}} = \mathbf{v}/|\mathbf{v}|$.) Suggestive contours are contours in nearby viewpoints, and three equivalent definitions were proposed in [DeCarlo et al. 2003] and extended for back-facing portions of the surface (where the sign of the derivative test is reversed when $\hat{\mathbf{n}} \cdot \hat{\mathbf{v}} < 0$) in [Burns et al. 2005]. The definition we will use here is in terms of the radial curvature κ_r, which is the curvature measured in the direction $\hat{\mathbf{w}}$. The direction $\hat{\mathbf{w}}$ is the normalized projection of the viewing direction $\mathbf{v}$ onto the tangent plane at $\mathbf{p}$. Thus, suggestive contours are defined as:

$$\kappa_r = 0 \quad \text{and} \quad \begin{cases} D_{\hat{\mathbf{w}}}\, \kappa_r > 0 & \text{where } \hat{\mathbf{n}} \cdot \hat{\mathbf{v}} > 0 \\ D_{\hat{\mathbf{w}}}\, \kappa_r < 0 & \text{where } \hat{\mathbf{n}} \cdot \hat{\mathbf{v}} < 0 \end{cases} \tag{2}$$

which is equivalent to positive minima (or negative maxima) of $\hat{\mathbf{n}} \cdot \mathbf{v}$ in the direction $\hat{\mathbf{w}}$.

Examples of surface locations on contours and suggestive contours are diagrammed in a side-view of a shape in Figure 2; contours (C) are those locations where the surface is viewed edge-on, and suggestive contours (SC) are inflections where the convex side is closer to the camera (on front-facing parts of the surface).

3.1 Mathematical Approach

This diagram also includes the two types of highlight lines: the suggestive highlight (SH) and the principal highlight (PH). The motivation for these lines is similar to the motivation for the image-space algorithm for suggestive contours [DeCarlo et al. 2003], which put suggestive contours in approximate correspondence to intensity valleys in images. Here we want to find features on the surface that roughly correspond to intensity *ridges* in images.

Ridges can be understood intuitively as regions where the surface changes quickly in one direction but is comparably flat in a sideways direction. The technical difficulty is to characterize these two directions in terms of geometrical quantities on the surface. Such an approach is in fact given by the definition of creases due to Saint-Venant [Koenderink and van Doorn 1993; Rieger 1997]. It uses second derivatives of the height field, computed in the gradient and perpendicular directions, to abstract changes in the surface in a general way. (Other definitions of ridges involve even higher-order derivatives.) This definition has been explored by Yuille [1989] and Rieger [1997], but is poorly suited to a direct object-space implementation because it requires finding zeroes of third derivatives of surface geometry (the image height field already tracks first-

derivative changes in the surface through $\hat{\mathbf{n}}$). What we will do instead is to attempt to catch most of the meaningful image ridges by looking for places where intensity changes quickly along either of the two natural directions for exploring a viewed surface: $\hat{\mathbf{w}}$, the projection of the view direction into the tangent plane of the surface; and $\hat{\mathbf{w}}_\perp$, the perpendicular to $\hat{\mathbf{w}}$ in the tangent plane. The first case leads to lines we call *suggestive highlights*, while the second case leads to lines we call *principal highlights*. These definitions prove simple enough to implement but are sufficiently grounded in the mathematics of shape to convey highlights effectively[1].

3.2 Suggestive Highlights

Suggestive highlights are complementary to suggestive contours: they are positive *maxima* (or negative *minima*) of $\hat{\mathbf{n}} \cdot \mathbf{v}$ in the direction $\hat{\mathbf{w}}$. Equivalently, these are locations at which:

$$\kappa_r = 0 \quad \text{and} \quad \begin{cases} D_{\hat{\mathbf{w}}}\,\kappa_r < 0 & \text{where } \hat{\mathbf{n}} \cdot \hat{\mathbf{v}} > 0 \\ D_{\hat{\mathbf{w}}}\,\kappa_r > 0 & \text{where } \hat{\mathbf{n}} \cdot \hat{\mathbf{v}} < 0 \end{cases} . \qquad (3)$$

(This is based on a derivation that is similar to that of suggestive contours.) In Figure 2 these points are labeled SH, and account for the remaining view-dependent inflections on the shape. Thus, suggestive highlights are simply the "other" part of the solution set of $\kappa_r = 0$. We will see in Section 5 how both suggestive contours and highlights can be used effectively in the same line drawing.

3.3 Principal Highlights

Principal highlights (PH) are strong positive maxima (or negative minima) of $\hat{\mathbf{n}} \cdot \mathbf{v}$ in the direction $\hat{\mathbf{w}}_\perp$. The direction $\hat{\mathbf{w}}_\perp = \hat{\mathbf{n}} \times \hat{\mathbf{w}}$ sits perpendicular to $\hat{\mathbf{w}}$ in the tangent plane [DeCarlo et al. 2004]. Deriving a definition of PH in terms of second derivative quantities is achieved by differentiating $\hat{\mathbf{n}} \cdot \mathbf{v}$ in the direction $\hat{\mathbf{w}}_\perp$ and setting it equal to zero. Maxima occur where the second derivative in this direction is negative.

The derivation proceeds along similar lines to that in [DeCarlo et al. 2003]. Beginning with the condition for extrema, locations where $D_{\hat{\mathbf{w}}_\perp}(\hat{\mathbf{n}} \cdot \mathbf{v}) = 0$, we can show that $D_{\hat{\mathbf{w}}_\perp}(\hat{\mathbf{n}} \cdot \mathbf{v}) = (D_{\hat{\mathbf{w}}_\perp}\hat{\mathbf{n}}) \cdot \mathbf{v} + \hat{\mathbf{n}} \cdot D_{\hat{\mathbf{w}}_\perp}\mathbf{v} = \mathrm{II}(\hat{\mathbf{w}}_\perp) \cdot \mathbf{v} + 0 = \mathrm{II}(\mathbf{w}, \hat{\mathbf{w}}_\perp) = \tau_r |\mathbf{w}|$, where τ_r is the radial torsion [DeCarlo et al. 2004]—the geodesic torsion in the direction $\hat{\mathbf{w}}$. For the time being, if we disregard locations where $\hat{\mathbf{n}}$ and $\mathbf{v}$ are parallel (where $\mathbf{w} = 0$), then it follows that principal highlights are in locations where $\tau_r = 0$ and $D_{\hat{\mathbf{w}}_\perp}\tau_r < 0$ (on front-facing parts of the shape).

We note that τ_r is zero at locations where $\hat{\mathbf{w}}$ lines up with either principal direction, $\mathbf{e}_1$ or $\mathbf{e}_2$, or where $\kappa_1 = \kappa_2$. (Here, we assume $|\kappa_1| \geq |\kappa_2|$.) Figure 3(a) shows the solution of $\tau_r = 0$ on a torus. If we consider only those cases in which $\hat{\mathbf{w}}$ lines up with $\mathbf{e}_2$, as drawn in Figure 3(b), we note that this corresponds to stronger maxima of $\hat{\mathbf{n}} \cdot \mathbf{v}$ than when $\hat{\mathbf{w}}$ lines up with $\mathbf{e}_1$: referring to the diffuse shading in Figure 3(d), we see that the variation in $\hat{\mathbf{n}} \cdot \hat{\mathbf{v}}$ is larger in the direction perpendicular to $\mathbf{e}_2 = \hat{\mathbf{w}}$. Thus, we restrict our definition of principal highlights to locations where $\hat{\mathbf{w}}$ lines up with $\mathbf{e}_2$, or $\hat{\mathbf{w}} \cdot \mathbf{e}_1 = 0$:

$$\hat{\mathbf{w}} \cdot \mathbf{e}_1 = 0 \quad \text{and} \quad \begin{cases} D_{\hat{\mathbf{w}}_\perp}\tau_r < 0 & \text{where } \hat{\mathbf{n}} \cdot \hat{\mathbf{v}} > 0 \\ D_{\hat{\mathbf{w}}_\perp}\tau_r > 0 & \text{where } \hat{\mathbf{n}} \cdot \hat{\mathbf{v}} < 0 \end{cases} . \qquad (4)$$

(We also add points at which $\mathbf{w} = 0$.)

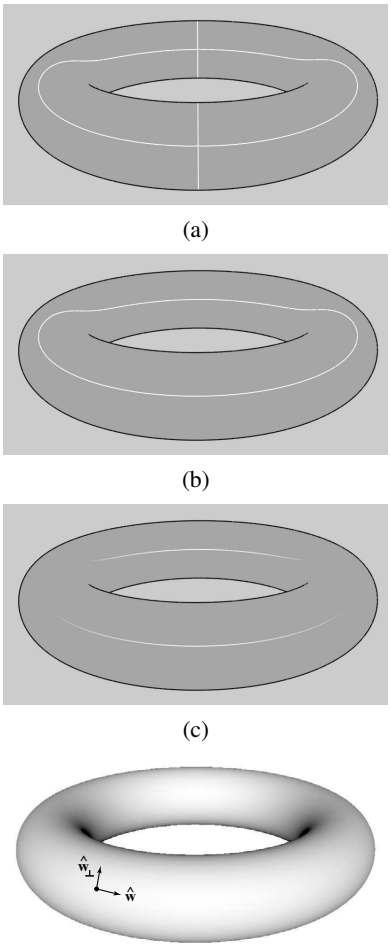

Figure 3: *(a) Locations with $\tau_r = 0$; (b) Locations where $\hat{\mathbf{w}}$ lines up with $\mathbf{e}_2$; (c) With derivative test applied; (d) Diffuse-shaded rendering of a torus.*

As with suggestive contours, we have found that we produce more stable and aesthetically pleasing drawings by changing the derivative tests to use a small positive constant ε rather than zero [DeCarlo et al. 2003], and by fading out lines as they approach the derivative threshold [DeCarlo et al. 2004]. Applying these effects results in the rendering in Figure 3(c).

It turns out that locations where $\hat{\mathbf{w}} \cdot \mathbf{e}_1 = 0$ are also (view-dependent) creases in the depth map. In other words, if we consider the surface as a height field as viewed from the camera, then these locations are exactly the ridges and valleys, using the particular definition due to Saint-Venant [Koenderink and van Doorn 1993]. A proof of this equivalence is presented in Appendix A. To avoid confusion, it is

[1] It is worth noting that we have considered positive *minima* of $\hat{\mathbf{n}} \cdot \hat{\mathbf{v}}$ in $\hat{\mathbf{w}}_\perp$ as well. Given these are on creases in depth (as shown below), these will rarely occur on front-facing parts of the surface. Empirically, we have noticed that while unusual, these do occur nearby locations where the Gaussian curvature is zero, and are generally redundant with suggestive contours. It seems safe to leave these out.

worth noting that these ridges and valleys in depth are distinct from (view-independent) ridges and valleys on the surface [Ohtake et al. 2004] and (view-dependent) apparent ridges on the surface [Judd et al. 2007], as well as from intensity ridges and valleys of the rendered image (i.e., interpreting the image intensity as "height") [Pearson and Robinson 1985; Iverson and Zucker 1995; Lee et al. 2007]. In the case of principal highlights, we can separate the cases based on the sign of κ_1 (which, as we have seen, is the curvature roughly perpendicular to the PH lines): ridges have positive κ_1, and valleys have negative κ_1. These correspond to the PH+ and PH– in Figure 2. We have found it helpful to treat them separately at rendering time, giving artistic control to the user to stylize them differently or omit one family (for many models, omitting the valleys results in less-cluttered drawings).

4 Computation

Suggestive Highlights: Computation of suggestive highlights is straightforward, and proceeds similarly to suggestive contours [DeCarlo et al. 2003]. We use a separate threshold on the derivative test, which in practice is set higher than for suggestive contours, to remove more of the shallow extrema.

Principal Highlights: As we saw in Figure 3(a), solving $\tau_r = 0$ leads to finding locations at which $\hat{\mathbf{w}} \cdot \mathbf{e}_1 = 0$, $\hat{\mathbf{w}} \cdot \mathbf{e}_2 = 0$, and $\kappa_1 = \kappa_2$. These can form overlapping loops on the surface. Even worse, the crossing points happen where $\hat{\mathbf{w}}$ is singular—locations where $\hat{\mathbf{n}} \cdot \hat{\mathbf{v}} = 1$. The presence of crossing loops leads to difficulty in extracting the lines using a simple per-triangle strategy of looking for zeros of τ_r interpolated from the corners. The artifacts are most obvious on coarsely sampled meshes, as shown in Figure 4. A better strategy is therefore to extract just the loops we need. However, if one solves for $\hat{\mathbf{w}} \cdot \mathbf{e}_1 = 0$ directly, the lack of consistency between the signs of $\mathbf{e}_1$ within a triangle causes serious problems—triangles may contain spurious sign flips due to this. A similar difficulty is encountered when extracting (geometric) ridges and valleys of surfaces, and so we can proceed similarly to the strategy adopted for the latter problem by Ohtake et al. [2004]. (An analogous strategy is also used for apparent ridges by Judd et al. [2007].)

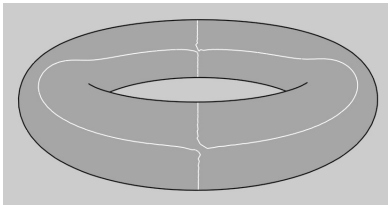

Figure 4: *Difficulties with naive extraction of $\tau_r = 0$ curves.*

When processing a triangle, we flip the directions of $\mathbf{e}_1$ at each of the vertices so they are all consistent with the vertex that has the largest value of κ_1. For triangles having $\kappa_1 \approx \kappa_2$—near an umbilic—this strategy may not work as $\mathbf{e}_1$ and $\mathbf{e}_2$ may have interchanged within a triangle. Fortunately, we can skip this case, as we are not interested in suggestive highlights near umbilics (they tend to produce "shallow" local maxima). We detect this situation by noting when the angle between the flipped $\mathbf{e}_1$ vector and the reference $\mathbf{e}_1$ exceeds 45 degrees.

We actually solve for zeros of $(\hat{\mathbf{w}} \cdot \mathbf{e}_1) \sin\theta = \hat{\mathbf{v}} \cdot \mathbf{e}_1$, as this avoids the singularities in $\hat{\mathbf{w}}$ (which also happen to be local maxima of $\hat{\mathbf{n}} \cdot \hat{\mathbf{v}}$, so we do want to include them). After this, computation proceeds normally. We ensure that we are extracting maxima by enforcing $-D_{\hat{\mathbf{w}}_\perp}\tau_r > \varepsilon_{ph} > 0$ for front-facing parts of the surface (where ε_{ph} is a threshold value to eliminate insignificant or noisy lines). Using derivation methods from [DeCarlo et al. 2004], one can show:

$$D_{\hat{\mathbf{w}}_\perp}\tau_r = C(\hat{\mathbf{w}}, \hat{\mathbf{w}}_\perp, \hat{\mathbf{w}}_\perp) - \cot\theta\,(2H - \kappa_r)(2H - 2\kappa_r) \quad (5)$$

$$= \pm D_{\mathbf{e}_2}\kappa_1 - \cot\theta\,\kappa_1(\kappa_1 - \kappa_2) \quad \text{when } \hat{\mathbf{w}} = \pm\mathbf{e}_2 \quad (6)$$

However, instead of this relatively complex test, we have found in practice that enforcing $(\kappa_1^2 - \kappa_2^2)\cos\theta > \varepsilon_{ph} > 0$ effectively removes the unwanted lines.

5 Rendering Styles

We have investigated a number of rendering styles that include contours, suggestive contours, suggestive highlights and principal highlights. We describe two of the more successful styles here.

Gray Background: The first style simply draws contours and suggestive contours in black, suggestive and principal highlights in white, all against a gray background. This style is quite effective, particularly on models without too many lines. Such an effect cannot be achieved just using a toon shader—see Figure 5. This style also combines productively with a toon shader, provided that the lightest and darkest tones do not hide the lines.

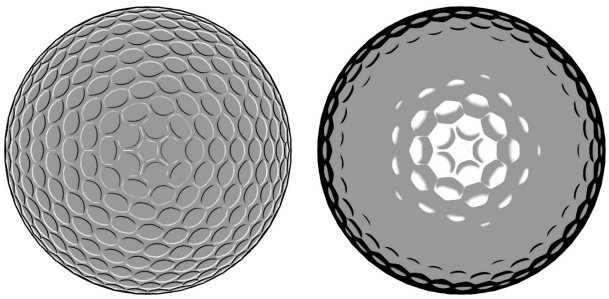

C + SC + SH + PH Toon shader

Figure 5: *A rendering with suggestive contours and both suggestive and principal highlights conveys details across the entire shape (left), unlike toon shading (right).*

There are cases, however, in which this style becomes less effective, such as when the two halves of the same $\kappa_r = 0$ loop are perceptually grouped together in a way that resembles embossing. Shape is still conveyed, but it does not appear to be the correct shape. An example is seen in the close-up of the armadillo leg in Figure 6. This effect is most noticeable when the lines are viewed up close, perhaps because at a distance the style is essentially a form of exaggerated shading [Rusinkiewicz et al. 2006], although using three discrete tone levels. Leaving out suggestive highlights (but still including principal highlights) avoids this effect. Figure 1 shows results with different types of highlight lines on the head of the David.

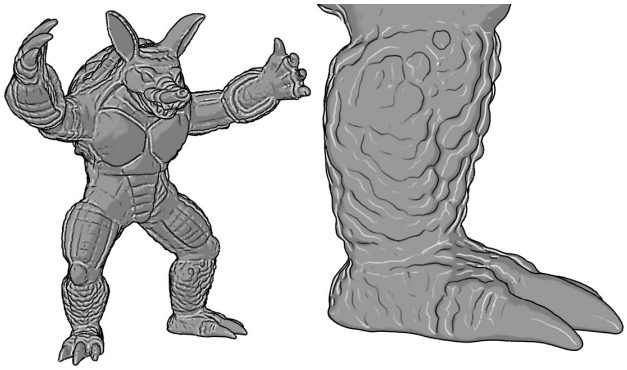

C + SC + SH + PH + toon shader Close-up of leg

Figure 6: *Armadillo in gray style. On the right, notice the incorrect embossed appearance that can result from rendering suggestive contours together with suggestive highlights.*

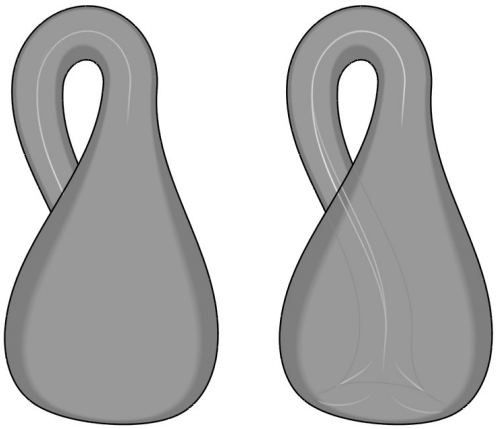

Figure 7: *A Klein bottle rendered both opaquely and transparently (C + SC + SH + PH)*

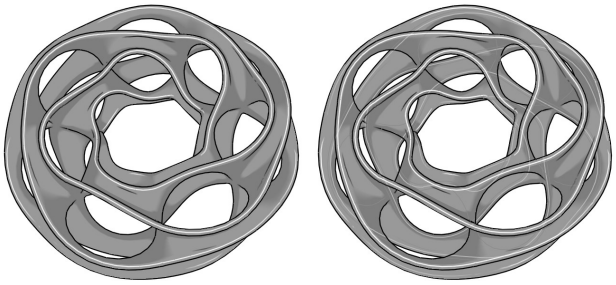

Figure 8: *The "Heptagonal Toroid" (by Brent Collins and Carlo Séquin) rendered both opaquely and transparently (C + SC + PH ridges)*

Using the definitions of lines on back-facing parts of the shape, it is straightforward to produce transparent renderings (in which hidden lines are drawn, faded by a fixed amount, in a separate pass). Figure 7 shows an example of this on a Klein bottle, and Figure 8 on the Heptagonal Toroid.

Shading in Black and White: The second style is inspired by the work of certain artists that work in black and white, such as the comic book creator Frank Miller. The image in Figure 9 is such an example, where the bricks are depicted while in shadow using white lines. Upon closer inspection (at right) it becomes clear that the white lines are in *different places* than the black lines: shadows are *not* simply negatives of lit areas. Thus, we draw suggestive contours in black, highlight lines in white, against a two-level toon shader that is black and white.

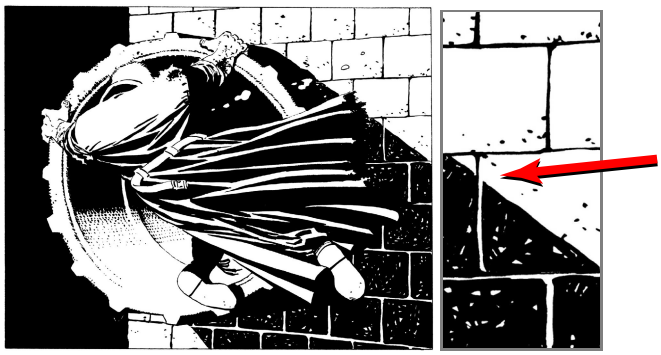

Figure 9: *Excerpt from Frank Miller's* Sin City, *©1991 Frank Miller, Inc. The white lines in the cast shadow depict shape that could not be revealed with black lines.*

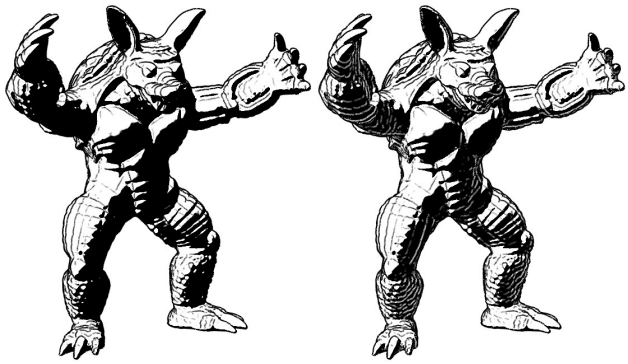

C + SC C + SC + SH

Figure 10: *In the black and white style, when suggestive highlights are included, the shape is conveyed in the dark areas.*

The result is more dramatic and less cluttered than the gray style mentioned earlier. The addition of the highlight lines fills out the dark regions, as can be seen by comparing the renderings with and without suggestive highlights in Figure 10. Our results also more closely resemble the lines drawn by Miller than the simple strategy of inverting dark regions, as was proposed by Spindler et al. [2006].

Off-center Light: It is also possible to adjust the definition of the lines to account for a changing light position (for suggestive contours and both types of highlight lines). We have experimented with simply replacing all of the $\hat{\mathbf{w}}$ and $\hat{\mathbf{w}}_{\perp}$ quantities in the line definitions with projections of the lighting direction (and its perpendicular). We have found this to be most effective on objects with many bumps and dimples. However, at times these lines can seem misplaced as they slide over a ridge, and more investigation on their behavior is warranted. Two examples are displayed in Figure 13.

6 Discussion and Conclusion

The renderings of golf balls in Figure 11 show how different types of lines contribute to an effective rendering. All renderings

include contours and suggestive contours, and the first row shows suggestive highlights rendered separately from principal highlights. The second row shows the effects when these lines are combined, first with a solid gray background, and then with a light toon shader.

Figure 12 shows a comparison between the painting "Golf Ball" by Roy Lichtenstein and renderings produced by our system. While our system does not reproduce all of the interesting aspects of design and stylization in this work, there are similarities: the upper part of the painting has lines that abstract dark areas, while in the shadow the lines abstract light areas. This compares well to a rendering in our black and white style, using suggestive contours in the light and suggestive highlights in the shadow. It is worth comparing the orientation of the curved lines that depict the dimples—they are the same in our rendering as in the painting. In contrast, we can simply draw suggestive contours in white in the shadowed areas (labeled inverse(SC) in the figure), which is comparable to the approach of Spindler et al. [2006]. This produces lines that disagree with Lichtenstein's and lead to a conflicted and ineffective rendering. We believe that this comparison provides one of the strongest arguments for this work.

Although SH and PH lines are not defined explicitly in terms of intensity ridges in the image, we have empirically observed that they typically occur near such ridges (much as suggestive contours typically occur near intensity valleys). We have adapted the image-space algorithm described by DeCarlo et al. [2003] for suggestive contours to extract both ridges and valleys of a diffusely rendered image. The changes are straightforward, with perhaps the most substantial being that the rendered diffuse images use $\frac{1}{2} + \frac{1}{2}(\hat{\mathbf{n}} \cdot \hat{\mathbf{l}})$, so that lines can still be extracted from locations in shadow. The results of the image space algorithm are provided for the golf ball—in Figure 11, and in Figure 13 with an off-center light. We believe that a better theoretical understanding of this relationship is in order, though this is future work.

In summary, we have presented two new types of lines that convey highlights—suggestive highlights and principal highlights. The lines are defined in a way that extends the concept of suggestive contours to local *maxima* of $\hat{\mathbf{n}} \cdot \mathbf{v}$, in the $\hat{\mathbf{w}}$ and $\hat{\mathbf{w}}_\perp$ directions. The lines can be effectively used in different styles, augmenting existing lines to convey more information about surface geometry.

Acknowledgments

We thank Hamilton Chong, Adam Finkelstein, Steven Gortler, Xiaofeng Mi, Manish Singh and Matthew Stone for their insights and helpful conversations. 3D models in this paper are courtesy of Stanford University, the Digital Michelangelo Project, and UC Berkeley, while Figure 12(left) is ©Estate of Roy Lichtenstein, and Figure 9 is ©Frank Miller, Inc. This work is partially supported by the National Science Foundation through grants CCF-0541185, CCF-0347427, and IIS-0511965, as well as the Sloan Foundation.

References

BURNS, M., KLAWE, J., RUSINKIEWICZ, S., FINKELSTEIN, A., AND DECARLO, D. 2005. Line drawings from volume data. *ACM Transactions on Graphics (Proc. SIGGRAPH) 24*, 3 (Aug.), 512–518.

CIPOLLA, R., AND GIBLIN, P. J. 2000. *Visual Motion of Curves and Surfaces*. Cambridge University Press.

DECARLO, D., FINKELSTEIN, A., RUSINKIEWICZ, S., AND SANTELLA, A. 2003. Suggestive contours for conveying shape. *ACM Transactions on Graphics (Proc. SIGGRAPH) 22*, 3, 848–855.

DECARLO, D., FINKELSTEIN, A., AND RUSINKIEWICZ, S. 2004. Interactive rendering of suggestive contours with temporal coherence. In *NPAR 2004: Proceedings of the 3rd international symposium on Non-photorealistic animation and rendering*, ACM Press, New York, NY, USA, 15–145.

ELBER, G., AND COHEN, E. 1990. Hidden curve removal for free form surfaces. In *Computer Graphics (Proceedings of SIGGRAPH 90)*, 95–104.

GOOCH, B., SLOAN, P.-P. J., GOOCH, A., SHIRLEY, P., AND RIESENFELD, R. 1999. Interactive technical illustration. In *SI3D '99: Proceedings of the 1999 symposium on Interactive 3D graphics*, ACM Press, New York, NY, USA, 31–38.

HERTZMANN, A., AND ZORIN, D. 2000. Illustrating smooth surfaces. In *Proceedings of ACM SIGGRAPH 2000*, Computer Graphics Proceedings, Annual Conference Series, 517–526.

INTERRANTE, V., FUCHS, H., AND PIZER, S. 1995. Enhancing transparent skin surfaces with ridge and valley lines. In *Proceedings of the 6th conference on Visualization '95*, IEEE Computer Society, Washington, DC, USA, 52–59.

IVERSON, L. A., AND ZUCKER, S. W. 1995. Logical/linear operators for image curves. *IEEE Transactions on Pattern Analysis and Machine Intelligence 17*, 10, 982–996.

JUDD, T., DURAND, F., AND ADELSON, E. 2007. Apparent ridges for line drawing. *ACM Transactions on Graphics (Proc. SIGGRAPH) 26*, 3, Article 19.

KOENDERINK, J., AND VAN DOORN, A. 1993. Local features of smooth shapes: Ridges and courses. *Proceedings of the SPIE 2031*, 2–13.

LEE, Y., MARKOSIAN, L., LEE, S., AND HUGHES, J. F. 2007. Line drawings via abstracted shading. *ACM Transactions on Graphics (Proc. SIGGRAPH) 26*, 3, Article 18.

MARKOSIAN, L., KOWALSKI, M. A., GOLDSTEIN, D., TRYCHIN, S. J., HUGHES, J. F., AND BOURDEV, L. D. 1997. Real-time nonphotorealistic rendering. In *SIGGRAPH '97: Proceedings of the 24th annual conference on Computer graphics and interactive techniques*, ACM Press/Addison-Wesley Publishing Co., New York, NY, USA, 415–420.

OHTAKE, Y., BELYAEV, A., AND SEIDEL, H.-P. 2004. Ridge-valley lines on meshes via implicit surface fitting. *ACM Transactions on Graphics 23*, 3 (Aug.), 609–612.

PAULY, M., KEISER, R., AND GROSS, M. 2003. Multi-scale feature extraction on point-sampled surfaces. *Computer Graphics Forum 22*, 3 (Sept.), 281–290.

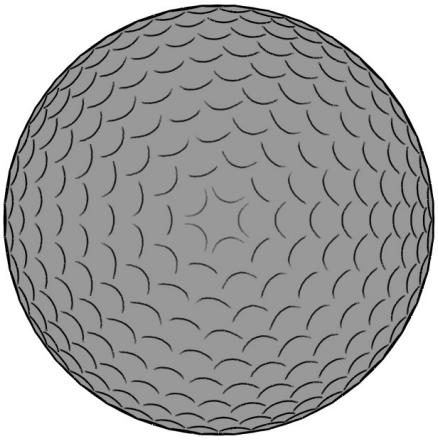

C + SC

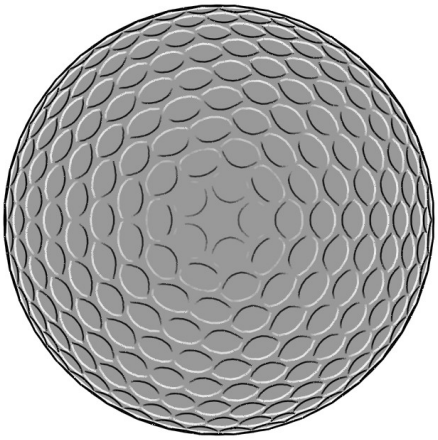

C + SC + SH

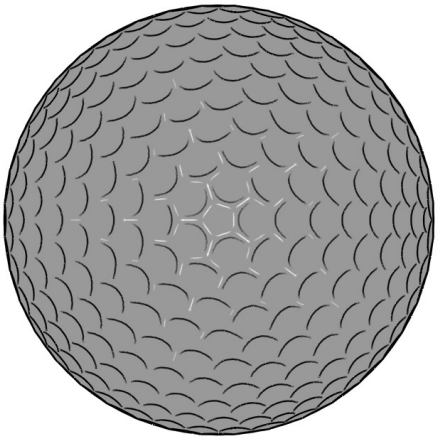

C + SC + PH

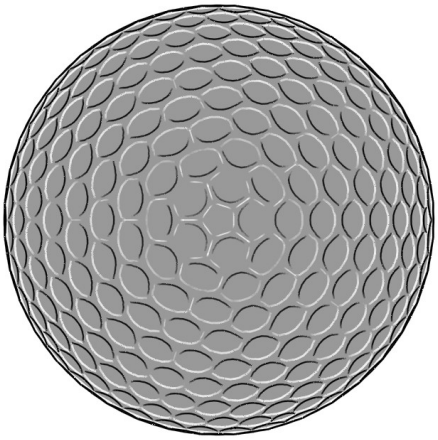

C + SC + SH + PH

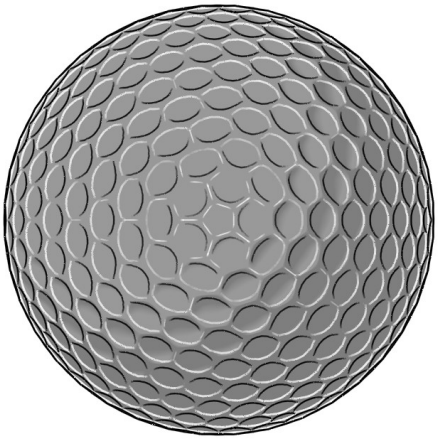

C + SC + SH + PH + toon

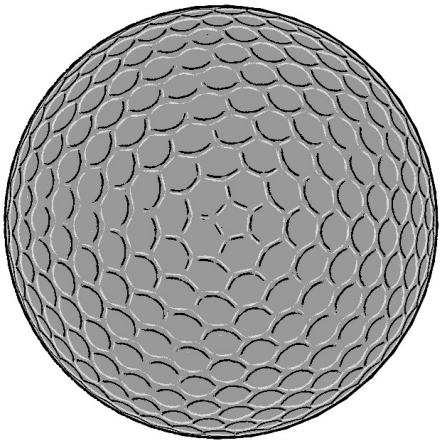

image space algorithm

Figure 11: *Golf balls in gray style*

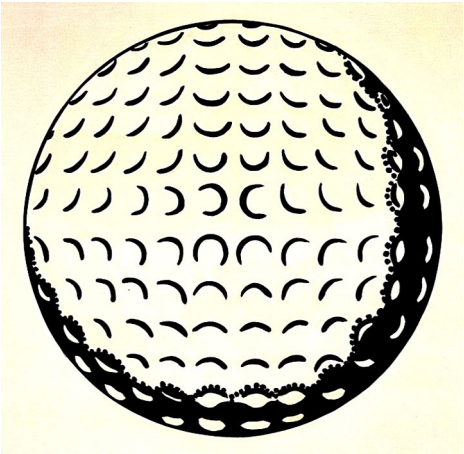

Roy Lichtenstein, “Golf Ball”, 1962
© Estate of Roy Lichtenstein

C + SC + SH

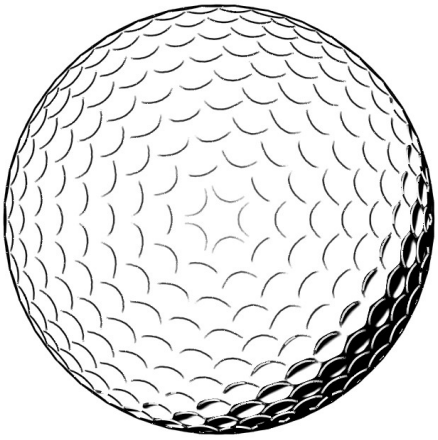

C + SC + inverse(SC)

Figure 12: *Golf balls in hard black and white style.*

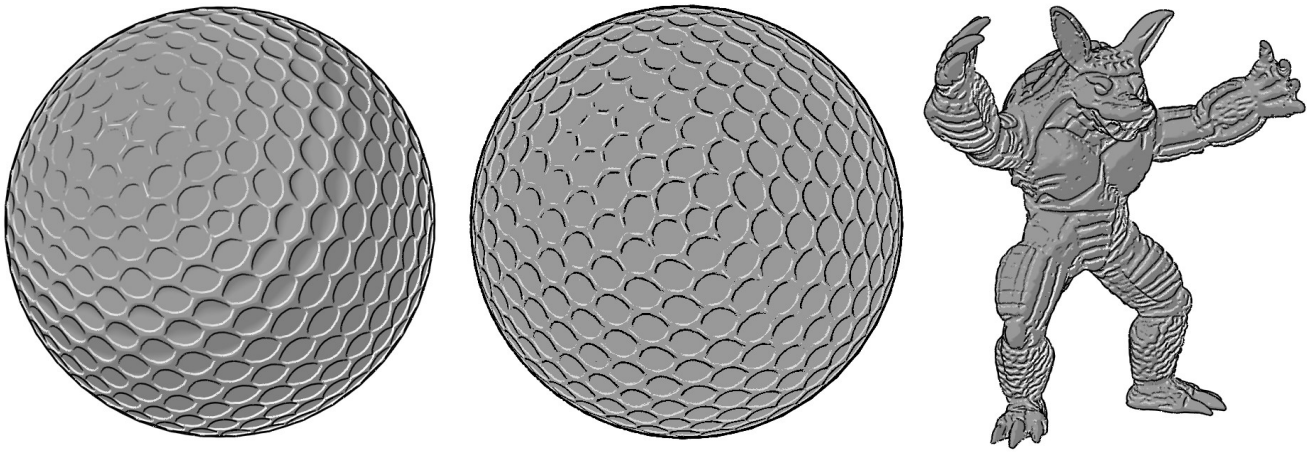

C + SC + SH + PH + toon (gray) image space algorithm C + SC + SH + PH + toon (gray)

Figure 13: *Renderings with an off-center light.*

PEARSON, D., AND ROBINSON, J. 1985. Visual communication at very low data rates. *Proceedings of the IEEE 4* (Apr.), 795–812.

RIEGER, J. H. 1997. Topographical properties of generic images. *International Journal of Computer Vision 23*, 1, 79–92.

RUSINKIEWICZ, S., BURNS, M., AND DECARLO, D. 2006. Exaggerated shading for depicting shape and detail. *ACM Transactions on Graphics 25*, 3 (July), 1199–1205.

SAITO, T., AND TAKAHASHI, T. 1990. Comprehensible rendering of 3-D shapes. In *Computer Graphics (Proceedings of SIGGRAPH 90)*, 197–206.

SPINDLER, M., RÖBER, N., DÖHRING, R., AND MASUCH, M. 2006. Enhanced cartoon and comic rendering. In *Proc. Eurographics Short Papers*, 141–144.

THIRION, J.-P., AND GOURDON, A. 1996. The 3D marching lines algorithm. *Graphical Models and Image Processing 58*, 6 (Nov.), 503–509.

WEIDENBACHER, U., BAYERL, P., NEUMANN, H., AND FLEMING, R. 2006. Sketching shiny surfaces: 3d shape extraction and depiction of specular surfaces. *ACM Trans. Appl. Percept. 3*, 3, 262–285.

WINKENBACH, G., AND SALESIN, D. H. 1994. Computer-generated pen-and-ink illustration. In *Proceedings of SIGGRAPH 94*, Computer Graphics Proceedings, Annual Conference Series, 91–100.

YUILLE, A. L. 1989. Zero crossings on lines of curvature. *Computer Vision, Graphics, and Image Processing 45*, 68–87.

A Principal Highlights and Creases in Depth

In this appendix, we show that principal highlights are equivalent to (view-dependent) ridges and valleys of the depth image. We begin by considering an arbitrary height field f with gradient direction $\hat{g}$ and its perpendicular $\hat{g}_\perp$. The Saint-Venant condition for a crease [Koenderink and van Doorn 1993] can be formulated in terms of the Hessian of the height, expressed in an orthonormal coordinate system of the normalized gradient $\hat{g}$ and its perpendicular $\hat{g}_\perp$:

$$H = \begin{bmatrix} f_{\hat{g}\hat{g}} & f_{\hat{g}\hat{g}_\perp} \\ f_{\hat{g}\hat{g}_\perp} & f_{\hat{g}_\perp\hat{g}_\perp} \end{bmatrix} \tag{7}$$

The entries in this matrix are second derivatives of the height. For instance, $f_{\hat{g}\hat{g}}$ is the second derivative in the gradient direction. (The quantity $f_{\hat{g}}$ is the first derivative in the gradient direction, which is simply the gradient magnitude.)

The Saint-Venant condition for a crease is:

$$f_{\hat{g}\hat{g}_\perp} = 0 \quad \text{and} \quad |f_{\hat{g}\hat{g}}| < |f_{\hat{g}_\perp\hat{g}_\perp}| \quad \text{and} \quad \begin{cases} \text{Valley:} \\ \quad f_{\hat{g}_\perp\hat{g}_\perp} > 0 \\ \textit{or} \\ \text{Ridge:} \\ \quad f_{\hat{g}_\perp\hat{g}_\perp} < 0 \end{cases} \tag{8}$$

To apply this to depth maps, we first need to compute $\hat{g}$. Given the viewing direction $\hat{\mathbf{v}}$, and its normalized projection $\hat{\mathbf{w}}$ onto the surface, the gradient of depth along $\hat{\mathbf{v}}$ is simply the unnormalized projection $\hat{\mathbf{w}}\sin\theta = \hat{\mathbf{v}} - \hat{\mathbf{n}}\cos\theta$, where θ is the angle between $\hat{\mathbf{n}}$ and $\hat{\mathbf{v}}$. The Hessian of the depth is:

$$\nabla g = \nabla(\hat{\mathbf{v}} - \hat{\mathbf{n}}\cos\theta) = 0 - \mathrm{II}\cos\theta + 0 = -\mathrm{II}\cos\theta$$

(Here we use an orthographic view assumption, so that $\nabla\hat{\mathbf{v}} = 0$, and note that that $\hat{\mathbf{n}}\cdot\nabla\cos\theta = 0$ because $\nabla\cos\theta$ is in the tangent plane.)

Thus, using $\hat{g} = \hat{\mathbf{w}}$ and $\hat{g}_\perp = \hat{\mathbf{w}}_\perp$, the location of the crease is $f_{\hat{g}\hat{g}_\perp} = -\mathrm{II}(\hat{\mathbf{w}}, \hat{\mathbf{w}}_\perp)\cos\theta = -\tau_r\cos\theta = 0$. Similarly, we can easily determine $f_{\hat{g}\hat{g}} = -\mathrm{II}(\hat{\mathbf{w}}, \hat{\mathbf{w}})\cos\theta = -\kappa_r\cos\theta$ and $f_{\hat{g}_\perp\hat{g}_\perp} = -\mathrm{II}(\hat{\mathbf{w}}_\perp, \hat{\mathbf{w}}_\perp)\cos\theta = -(2H - \kappa_r)\cos\theta$ where $2H - \kappa_r$ is simply the curvature measured in the direction $\hat{\mathbf{w}}_\perp$.

Working out the condition $|f_{\hat{g}\hat{g}}| < |f_{\hat{g}_\perp\hat{g}_\perp}|$ by canceling the $\cos\theta$ and substituting leads to $|\kappa_r| < |2H - \kappa_r|$, which excludes the case where $\hat{\mathbf{w}}\cdot\mathbf{e}_2 = 0$. Thus, these creases are equivalent to $\hat{\mathbf{w}}\cdot\mathbf{e}_1 = 0$. The classification into a ridge or valley is simply based on the sign of $-(2H - \kappa_r)\cos\theta$, which matches our intuition that κ_1 is positive on a ridge, and negative on a valley (as depicted in Figure 2).